Effects of isotope substitution on local heating and inelastic current in hydrogen molecular junctions

Yu-Chang Chen*
Department of Electrophysics, National Chiao Tung University, 1001 Ta Hsueh Road, Hsinchu 30010, Taiwan
(Received 22 October 2008; published 12 December 2008)

Using first-principles approaches, we investigate the inelastic features in the hydrogen molecular junction. We observe that local heating and inelastic current have significant isotope-substitution effects. The junction instability is also relevant to the isotope substitution. We predict that the HD junction has the smallest breakdown voltage compared with the H_2 and D_2 junction in the optimized geometry. The selection rule for modes that significantly contribute to the inelastic effects is related to the component of vibration along the direction of electron transport.

DOI: 10.1103/PhysRevB.78.233310 PACS number(s): 73.63.Nm, 68.37.Ef, 73.40.Jn

Building electronic circuits from molecules is an inspiring idea.[1] In the past decade, motivated by this revolutionary idea, intensive theoretical and experimental studies have been conducted to explore the charge transport in a single molecule junction. Single molecule junction is the basic building block for electronic components in molecular electronics. Understanding the transport properties of the basic building block is of key importance in the design of a new form of electronic circuit at the atomic and molecular levels.[2–5]

The hydrogen junction is an ideal testbed to compare theories and experiments. Despite the simplicity of the hydrogen junction, the data reported for the conductance varying from 0.2 to 1.0 G_0 have provoked controversy.[6–11] The problem of inelastic electron-vibration interactions remains unsettled. For example, the features of current-voltage characteristics at a bias around 65 mV are attributed to the electron-vibration interactions.[8,12] However, a theoretical group has reported calculations to support the idea that the static atomic structure can still cause a pronounced resonance at this bias.[6] The mode identification and the selection rule for modes that significantly contributed to the inelastic electron-tunneling spectroscopy (IETS) have not reached unanimity. The identification of the spike in dI/dV at the Pt-H_2 system as the transverse vibration mode is still controversial.[13]

To clarify the fundamental inelastic electron-transport properties, we performed comparative studies on inelastic profiles among the H_2, HD, and D_2 junctions. The simplicity of the hydrogen junction allows the inelastic profiles to provide clear information for understanding how the vibration modes contribute to inelastic effects in the nanoscale junction. Owing to the small mass of the hydrogen atom, isotope substitution has a great influence on inelastic effects. While the isotope substitution does not affect the contact geometry and the bonding strength, it can serve as a controllable factor that is sensitive enough to explore the fundamental properties of inelastic effects in the nanoscale junction. Moreover, the vibrations excited before the breakdown voltage of the hydrogen junction are acousticlike modes connected to contact geometry and bonding strength. This is in sharp contrast to the IETS and high-resolution electron-energy-loss spectroscopy (HREELS) in the alkyle junction where all observed modes in experiments are optical-like modes more relevant to internal vibrations of the molecule.[14–20] As such, inelastic profiles in the hydrogen junction can provide more information on contact geometry and bonding strength in the molecular junctions. Although heating is an important effect relevant to the stability and performance of device, very few attempts have been made that addressed the nanojunction.[21]

In our results, we observed interesting inelastic features in the hydrogen junction. In the optimized geometry [Fig. 1(a)], the electron-vibration interaction is suppressed by the mass of the molecule. The electron-vibration interaction is found to be enhanced by asymmetric molecule, which leads to the most prominent heating and inelastic correction to the current in the HD junction. Since the current-induced force, irrelevant to the isotope substitution, is found to be small, we predict that the HD junction is the most unstable owing to local heating as the major breakdown mechanism. This feature can be verified by experiments. In a possible rotated geometry as shown in Fig. 1(b), we observe that all modes

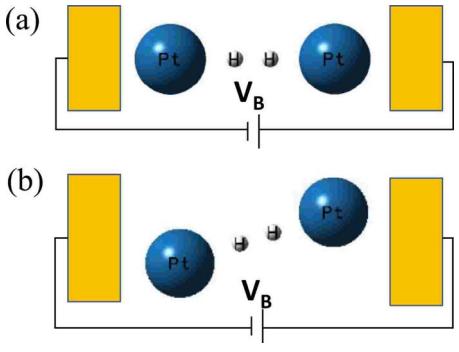

FIG. 1. (Color online) Schematic for the systems investigated. (a) The optimized geometry of the H_2 junction. The Pt-H-H-Pt atoms are sandwiched between two bulk Pt electrodes kept at a certain external bias with the chemical potentials of the left/right electrodes shifted; i.e., the source drain bias is $V_{SD}=(E_{FR}-E_{FL})/e$. The Pt electrodes are described as Jellium model with the interior electron density of Pt electrodes taken close to the value of metallic Pt ($r_s \approx 3$). The H-H, Pt-H, and Pt-Jellium distances are 1.615, 4.051, and 2.0 a.u., respectively. (b) A specific geometry of the H_2 junction. The hydrogen molecule rotates at an angle of 15° due to asymmetric contacts.

significantly contribute to inelastic profiles. It further confirms that the selection rule of important modes in the inelastic profiles is connected to the component of molecule vibration along the direction of charge transport. Thus, inelastic profile can be a sensitive tool to probe the contact geometry and bonding strength in the nanoscale junction.

We will begin our discussion by considering the inelastic current and heating effects in the linear hydrogen junction [Fig. 1(a)]. We study these effects by the first-order perturbation theory based on the second-quantized formalism where the wave functions are obtained from density-functional theory (DFT).[22] The scattering wave functions of the whole system are calculated by solving the Lippmann-Schwinger equation iteratively until the self-consistency is obtained.[23] The exchange and correlation energy is calculated at the level of the local-density approximation.[24] These wave functions are applied to calculate current and heating. The heating phenomenon in nanojunctions has been measured experimentally in the alkane junctions in a modified conducting atomic force microscopy (C-AFM), and the data are in reasonable agreement with our theoretical calculations.[21,25]

At first glance, the conductance of the hydrogen molecule is expected to be small because of a closed-shell configuration. However, the hybridization of states between hydrogen and Pt atoms can create new channel for current.[7] As a result, the magnitude of conductance, irrelevant to the isotope substitution, can be quite large around 1.0 G_0 in the hydrogen junction. This feature is verified by the analysis of partial density of states (DOS). In our results, the current-voltage characteristic in the Pt-H-H-Pt junction is quite linear, with a conductance around $G \approx 0.9\ G_0$. We find that the s-wave state, mostly contributed by the hydrogen atoms, has negligible contribution to the conducting state. This feature supports the argument that the origin of charge transport comes mainly from the H-Pt hybridized states.[7]

We briefly introduce the theory of the electron-vibration interactions. By applying the field operator with the wave functions obtained from the static DFT, the electron-vibration interaction has a second-quantized form,[22]

$$H_{\text{el-vib}} = \sum_{\alpha,\beta,E_1,E_2,j,\nu} \left(\sum_{i,\mu} \sqrt{\frac{\hbar}{2M_i\omega_{j\nu}}} A_{i\mu,j\nu} J^{i\mu,\alpha\beta}_{E_1,E_2} \right) \times a^{\alpha\dagger}_{E_1} a^{\beta}_{E_2} (b_{j\nu} + b^{\dagger}_{j\nu}), \quad (1)$$

where M_i is the mass of the ith atom, $A_{i\mu,j\nu}$ is a canonical transformation between normal coordinates and Cartesian coordinates satisfying $\Sigma_{i,\mu} A_{i\mu,j\nu} A_{i\mu,j'\nu'} = \delta_{j,j'}\delta_{\nu,\nu'}$; $J^{i\mu,\alpha\beta}_{E_1,E_2}$ is the coupling constant related to the electron and vibration of atoms, which can be calculated from the pseudopotential of atoms and wave functions, $a^{(L,R)}_{E}$ is the annihilation operator for an electron with energy E incident from the left or right electrode, respectively, $\hbar\omega_{j\nu}$ represents the energy of the $j\nu$th normal mode, and $b_{j\nu}$ is the annihilation operator corresponding to that mode. The strength of electron-vibration coupling is affected by the isotope substitution related to the mass of the molecule shown in Eq. (1).

TABLE I. Vibration modes depicted in Fig. 2. The unit of energies is in meV.

Modes	ω_{H_2}	ω_{HD} $(\frac{\omega_{H_2}}{\omega_{HD}})$	ω_{D_2} $(\frac{\omega_{H_2}}{\omega_{D_2}})$	Features
1	36.8	30.0(1.22)	26.1(1.41)	Transverse
2	36.8	30.0(1.22)	26.1(1.41)	Transverse
3	64.8	52.9(1.22)	45.9(1.41)	Longitudinal
4	115.9	101.1(1.15)	82.1(1.41)	Transverse
5	115.9	101.1(1.15)	82.1(1.41)	Transverse
6	314.9	273.4(1.15)	222.7(1.41)	Longitudinal

As the first step in our analysis, we focus on inelastic profiles in an optimized linear geometry as shown in Fig. 1(a). Two heavy Pt electrodes, which are inert owing to heavy masses, are simulated as two Pt atoms with infinite mass for simplicity. The geometry is relaxed in GAUSSIAN03 with the total energy of the system around −380.15 hartree. The geometry is stable and requires 0.53 eV to take the H_2 molecule away from the junction. In Table I, we list the energies of all the modes, while the schematics of vibrations for the H_2 molecule are shown in Fig. 2. Mode 3 is the one responsible for significant inelastic current and heating because of its longitudinal nature. Mode 6 is associated with a longitudinal internal vibration. The energy of this mode is too large to be excited before the breakdown bias around 200 mV found in experiments.[8,26] The rest of the modes have insignificant inelastic effects owing to their transverse natures.

In the linear hydrogen junction, the position of the discontinuities in the differential conductance is affected by the isotope substitution as shown in the upper panel of Fig. 3. In the H_2 junction, an abrupt change in the differential conductance appears at a bias around 65 mV in the d^2I/dV^2 spectrum. This peak is associated with mode 3 which has longitudinal character. This mode is associated with motion of the molecule as a rigid body. Accordingly, the energies are per-

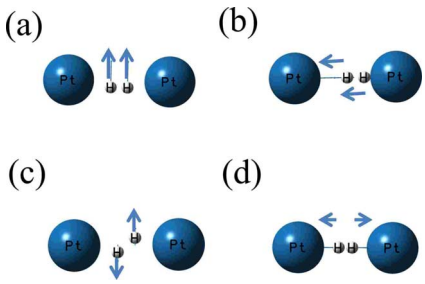

FIG. 2. (Color online) Schematic for the vibrational modes of the H_2 molecule. Six vibrational modes are shown in (a) for the modes 1 and 2 associated with a rigid motion of the H_2 molecule perpendicular to the line connecting two Pt atoms, (b) for the mode 3 associated with a rigid motion of the H_2 molecule along the line connecting Pt atoms, (c) for the modes 4 and 5 associated with a transverse motions of the H atoms, and (d) for the mode 6 associated with an internal vibration in H_2 along the line connecting Pt atoms. The energies and vibration characteristics of these modes are shown in Table I for the linear junction with a geometry depicted in Fig. 1(a).

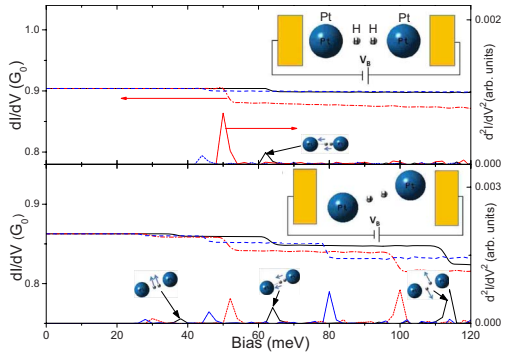

FIG. 3. (Color online) Differential conductance (left axis) and absolute value of d^2I/dV^2 (right axis) as a function of bias for the H_2 (black solid line), HD (red/gray dotted-dashed line), and D_2 (blue/dark gray dashed line) molecules sandwiched between the optimized linear junction (upper panel) and the junction of with asymmetric contacts (lower panel). The schematics show the noticeable modes contributed to the inelastic current in the H_2 junction.

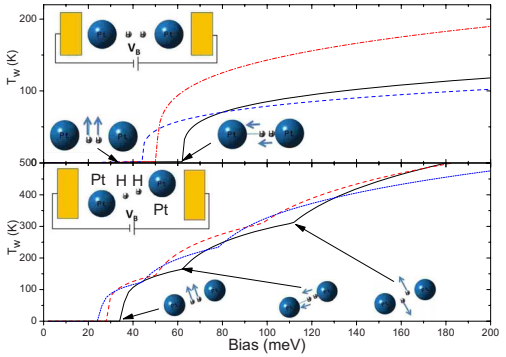

FIG. 4. (Color online) Local temperature as a function of bias for the H_2 (black solid line), HD (red/gray dotted-dashed line), and D_2 (blue/dark gray dashed line) molecules sandwiched between the optimized linear junction (upper panel) and the junction with asymmetric contacts (lower panel). The schematics show the noticeable modes contributed to heating in the H_2 junction.

fectly scaled by $\omega_{H_2}/\omega_{HD} \propto \sqrt{m_{HD}/m_{H_2}} \approx 1.22$. The rest modes with transverse characters are too weak to be resolved.

The magnitude of electron-vibration interaction is also affected by the isotope substitution. Let us compare the magnitude of discontinuities in the differential conductance in the linear H_2 and D_2 junctions. These two junctions have the same mechanical structures except for different masses. The electron-vibration coupling is related to the mass of ions by $1/\sqrt{M_i}$. Thus, the H_2 junction has a larger discontinuity in the differential conductance because of smaller mass. In the HD junction, the electron-vibration interaction is enhanced by asymmetric mass distribution. As a result, the HD junction has the largest change in the differential conductance.

Local temperatures in the linear H_2, HD, and D_2 junctions are further investigated to elucidate the role of isotope substitution. Two major processes lead to an equilibrium local temperature in a nanojunction. One is due to the electron-vibration interaction that occurs in the atomic region of the junction; the other is due to the dissipation of heat energy to the bulk electrodes via thermal transport.[27] We assume that the energy generated in the atomic region via inelastic electron-vibration scattering and the energy dissipated to the electrodes via thermal current finally reach equilibrium, such that a well-defined local temperature can be calculated in the atomic region. We evaluate the probability of the energy exchange via electron-vibration interactions by the Fermi golden rule for the four first-order scattering mechanisms. These mechanisms correspond to electrons incident from the right or left electrode that relax (cool) or excite (heat) the energy level of the normal-mode vibrations in the atomic region. The total thermal power generated in the junction can be calculated as the sum of all vibrational modes of the above four scattering mechanisms. Detailed theories can be found in Ref. 22.

Heating induced by the electron-electron interaction is neglected in present work since the contribution might be small compared with the electron-vibration interaction at small biases.[21,28] In the upper panel of Fig. 4 we plot the equilibrium temperature of the molecule as a function of applied voltage in the linear H_2, HD, and D_2 junctions. Weak heating phenomena occur at small biases corresponding to modes 1 and 2. These modes have very small contribution to heating due to their transverse vibration characters. Major heating profiles are observed at onset biases around 64.8, 52.8, and 45.9 mV for the H_2, HD and D_2 junctions, respectively. Those heating profiles are related to mode 3 with longitudinal vibration character.

The interplay between the onset bias and the strength of electron-vibration interaction caused by the isotope substitution leads to interesting heating profiles. For symmetric molecules in the linear junction [Fig. 1(a)], the magnitude of electron-vibration coupling is enhanced by the smaller mass (the H_2 junction) which leads to a larger heating rate, whereas the molecule with a larger mass (the D_2 junction) has a smaller onset bias. Consequently, a crossing in the equilibrium temperatures for the H_2 and D_2 junctions occurs at 80 mV as shown in the upper panel of Fig. 4. For the biases smaller than 80 mV, the local temperature in the D_2 junction is larger due to a smaller onset bias. For the biases larger than 80 mV, the local temperature in the H_2 junction is larger due to the larger electron-vibration coupling. For the HD junction, the asymmetric mass distribution leads to the enhancement of electron-vibration interaction. It accordingly induces the largest heating rate after the longitudinal normal mode is excited.

The junction stability is also relevant to isotope substitution. In atomic-sized Al wires, the current-induced force is the major mechanism that causes mechanical breaking, whereas in alkane junctions heating is the dominant breaking mechanism.[22,29] In our results, the current-induced forces on the hydrogen atoms have a small value of 0.38 nN at 200 mV. We thus expect that the major breakdown mechanism will be caused by local heating rather than the current-induced force. Because local heating is susceptible to effects of isotope substitution in contrast to the current-induced force where the isotope substitution plays no role, in the optimized geometry [Fig. 1(a)], we predict that compared with the H_2 and D_2 junctions, the HD junction has the smallest breakdown voltage caused by the most prominent heating.

As the detailed configurations in the contact region are unknown in the real experiment, the optimization of contact is not our present concern. We will concentrate on how the orientation of the molecule affects the inelastic profiles. We may now proceed to consider a specific configuration of the hydrogen junction where the hydrogen molecule rotated at an angle of 15° as shown in Fig. 1(b). The modes with transverse characters in the linear junction turn out to have large component of vibration along the direction of current in rotated geometry. The responses of inelastic current and local heating to the biases are shown in the lower panels of Figs. 3 and 4, respectively. In contrast to the optimized case [Fig. 1(a)] where only mode 3 had significant contribution to inelastic effects, all modes that can be excited cause prominent features in the inelastic profiles. These features further illustrate the selection rule for modes that significantly contribute to the inelastic effects related to the component of vibration along the direction of electron transport.

In conclusion, we have calculated various transport properties in H_2, HD, and D_2 molecular junctions in linear and rotated geometries. In the linear geometry, the *I-V* characteristics are linear with conductance $G \approx 0.9\ G_0$. We investigate how the isotope substitution can influence the inelastic current and local heating. The interplay between vibration energies and the electron-vibration coupling strength leads to interesting heating profile. We predict that the HD junction has the smallest breakdown voltage due to the enhancement of electron-vibration interaction. This feature is measurable and could give an insight into the mechanisms responsible for the system breakdown. We also investigate the inelastic effects in rotated geometry. The inelastic features further illustrate the selection rule for modes that significantly contribute to the inelastic effects related to the component of vibration along the direction of electron transport.

I am grateful to M. Di Ventra, M. Chshiev, and C. S. Chu for helpful discussions. This work was supported by Taiwan NSC under Contract No. 96-2112-M-009-037, MOE ATU, NCTS, and computing resources from NCHC.

*yuchangchen@mail.nctu.edu.tw

[1] A. Aviram and M. A. Ratner, Chem. Phys. Lett. **29**, 277 (1974).
[2] M. A. Reed, C. Zhou, C. J. Muller, T. P. Burgin, and J. M. Tour, Science **278**, 252 (1997).
[3] N. J. Tao, Nat. Nanotechnol. **1**, 173 (2006).
[4] S. M. Lindsay and M. A. Ratner, Adv. Mater. (Weinheim, Ger.) **19**, 23 (2007).
[5] M. Galperin, M. A. Ratner, A. Nitzan, and A. Troisi, Science **319**, 1056 (2008).
[6] Y. Qi, D. Guan, Y. Jiang, C. Liu, and D. Zhang, Appl. Phys. Lett. **89**, 182119 (2006).
[7] K. S. Thygesen and K. W. Jacobsen, Phys. Rev. Lett. **94**, 036807 (2005).
[8] R. H. M. Smit, Y. Noat, C. Untiedt, N. D. Lang, M. C. van Hemert, and J. M. van Ruitenbeek, Nature (London) **419**, 906 (2002).
[9] J. C. Cuevas, J. Heurich, F. Pauly, W. Wenzel, and G. Schön, Nanotechnology **14**, R29 (2003).
[10] Y. García, J. J. Palacios, E. SanFabián, J. A. Vergés, A. J. Pérez-Jiménez, and E. Louis, Phys. Rev. B **69**, 041402(R) (2004).
[11] Sz. Csonka, A. Halbritter, and G. Mihály, Phys. Rev. B **73**, 075405 (2006).
[12] D. Djukic and J. M. van Ruitenbeek, Nano Lett. **6**, 789 (2006).
[13] D. Djukic, K. S. Thygesen, C. Untiedt, R. H. M. Smit, K. W. Jacobsen, and J. M. van Ruitenbeek, Phys. Rev. B **71**, 161402(R) (2005).
[14] W. Wang, T. Lee, I. Kretzschmar, and M. A. Read, Nano Lett. **4**, 643 (2004).
[15] M. Galperin, M. A. Ratner, and A. Nitzan, J. Chem. Phys. **121**, 11965 (2004).
[16] J. Jiang, M. Kula, W. Lu, and Y. Luo, Nano Lett. **5**, 1551 (2005).
[17] L. H. Yu, C. D. Zangmeister, and J. G. Kushmerick, Phys. Rev. Lett. **98**, 206803 (2007).
[18] M. Paulsson, T. Frederiksen, and M. Brandbyge, Nano Lett. **6**, 258 (2006).
[19] G. C. Slomon, A. Gagliardi, A. Pecchia, T. Frauenheim, A. Di Carlo, J. R. Reimers, and N. S. Hush, J. Chem. Phys. **124**, 094704 (2006).
[20] J. G. Kushmerick, J. Lazorcik, C. H. Patterson, and R. Shashidhar, Nano Lett. **4**, 639 (2004); H. S. Kato, J. Noh, M. Hara, and M. Kawai, J. Phys. Chem. B **106**, 9655 (2002).
[21] Z. Huang, F. Chen, R. D'Agosta, P. A. Bennett, M. Di Ventra, and N. J. Tao, Nat. Nanotechnol. **2**, 698 (2007).
[22] Y.-C. Chen, M. Zwolak, and M. Di Ventra, Nano Lett. **3**, 1691 (2003); **4**, 1709 (2004); **5**, 621 (2005).
[23] N. D. Lang, Phys. Rev. B **52**, 5335 (1995); M. Di Ventra and N. D. Lang, *ibid.* **65**, 045402 (2001).
[24] Density-functional theory in local-density approximation may underestimate the highest occupied molecular orbital (HOMO)-lowest unoccupied molecular orbital (LUMO) gap for certain molecules. Quantitative description may not be accurate for insulating molecule. However, the hydrogen junction is in conducting state which lies in the reliable regime that the current approach can be applied.
[25] Z. Huang, B. Xu, Y.-C. Chen, M. Di Ventra, and N. J. Tao, Nano Lett. **6**, 1240 (2006).
[26] We employed the GAUSSIAN03 program to evaluate the vibrational modes of H_2, D_2, and HD molecule bonding to two Pt atoms at DFT level.
[27] We estimated the thermal current to dissipate the heat to electrodes following the weak link model by K. R. Patton and M. R. Geller, Phys. Rev. B **64**, 155320 (2001). The Young's modulus $Y \approx 2.748 \times 10^{11}$ dyne/cm^2 was calculated with total-energy calculations. We selected the effective length and effective cross section as $l \approx 1.86$ a.u. and $A \approx 3.14$ (a.u.)^2, respectively. Although these parameters may quantitatively affect the magnitude of thermal current, the features of local heating are highly consistent within the reasonable range of tunable parameters. The spectral densities were estimated from the dispersion relation of the surface phonon in Pt: $v_L \approx 3.60 \times 10^5$ cm/s and $v_T \approx 1.78 \times 10^5$ cm/s; see, for example, S. Hong, T. S. Rahman, R. Heid, and K. P. Bohnen, *ibid.* **71**, 245409 (2005).
[28] R. D'Agosta, N. Sai, and M. Di Ventra, Nano Lett. **6**, 2935 (2006).
[29] Z. Yang, M. Chshiev, M. Zwolak, Y.-C. Chen, and M. Di Ventra, Phys. Rev. B **71**, 041402(R) (2005).